aptara | NYAS | nyas_04332-1426019 | Dispatch: 1-4-2009 | CE: N/A
Journal | MSP No. | No. of pages: 17 | PE: Amanda/Carey

Numerical Investigation of Bubble Induced Marangoni Convection

Séamus M. O'Shaughnessy and Anthony J. Robinson

Department of Mechanical & Manufacturing Engineering, Trinity College Dublin, Ireland

The liquid motion induced by surface tension variation, termed the thermocapillary or Marangoni effect, and its contribution to boiling heat transfer has long been a very controversial issue. In the past this convection was not the subject of much attention because, under terrestrial conditions, it is superimposed by the strong buoyancy convection, which makes it difficult to obtain quantitative experimental results. The scenario under consideration in this paper may be applicable to the analysis of boiling heat transfer, specifically the bubble waiting period and, possibly, the bubble growth period. To elucidate the influence of Marangoni convection on local heat transfer, this work numerically investigates the presence of a hemispherical bubble of constant radius, $R_b = 1.0$ mm, situated on a heated wall immersed in a liquid silicone oil ($Pr = 82.5$) layer of constant depth $H = 5.0$ mm. A comprehensive description of the flow driven by surface tension gradients along the liquid–vapor interface required the solution of the nonlinear equations of free-surface hydrodynamics. For this problem, the procedure involved solution of the coupled equations of fluid mechanics and heat transfer using the finite-difference numerical technique. Simulations were carried out under zero-gravity conditions for temperatures of 50, 40, 30, 20, 10, and 1 K, corresponding to Marangoni numbers of 915, 732, 550, 366, 183, and 18.3, respectively. The predicted thermal and flow fields have been used to describe the enhancement of the heat transfer as a result of thermocapillary convection around a stationary bubble maintained on a heated surface. It was found that the heat transfer enhancement, as quantified by both the radius of enhancement and the ratio of Marangoni heat transfer to that of pure molecular diffusion, increases asymptotically with increasing Marangoni number. For the range of Marangoni numbers tested, a 1.18-fold improvement in the heat transfer was predicted within the region of $R_b \le r \le 7R_b$.

Key words: **Marangoni; thermocapillary; convection; bubble; microgravity; heat transfer; numerical**

Nomenclature

Bo	Bond number
C_p	specific heat [J·kg^{-1}K^{-1}]
H	liquid layer height [m]
k	thermal conductivity [W·m^{-1}K^{-1}]
Ma	Marangoni number
n	unit normal vector
p	pressure [N·m^{-2}]
Pr	Prandtl number
q''	heat flux [W·m^{-2}]
r	radial direction [m]
R_b	bubble radius [m]
R_{eff}	effective radius [m]
$R_{enhancement}$	enhancement radius [m]
T	temperature [K]
v	velocity [m·s^{-1}]
x	axial direction [m]

Greek Symbols

α	thermal diffusivity [m^2·s^{-1}]
Δ	difference
θ	azimuthal direction [rad]
μ	dynamic viscosity [kg·m^{-1}s^{-1}]
ρ	density [kg·m^{-3}]

Address for correspondence: Dr. Anthony J. Robinson, Department of Mechanical & Manufacturing Engineering, Parsons Building, Trinity College, Dublin 2, Ireland. Voice: +353 1 896 3919. arobins@tcd.ie

Interdisciplinary Transport Phenomena V: Ann. N.Y. Acad. Sci. xxxx: 1–17 (2009).
doi: 10.1111/j.1749-6632.2008.04332.x

σ	surface tension [$N \cdot m^{-1}$]
τ	shear stress [$N \cdot m^{-2}$]
υ	kinematic viscosity [$m^2 \cdot s^{-1}$]

Subscripts

2D	two-dimensional
3D	three-dimensional
c	cold side
cond	conduction
crit	critical point property
h	hot side
Ma	Marangoni
oil	oil property
r	radial
w	wall
x	axial

Introduction

Most natural convection processes in terrestrial environments are buoyancy driven and caused by unstable density gradients that are due to temperature differences within the system.[1] The presence of a liquid–vapor interface subject to a temperature gradient can initiate another form of natural convection, which is independent of gravitational acceleration and therefore the only natural convection mechanism for microgravity applications. This other mode of convection is dependent on surface tension variations with temperature and is termed thermocapillary convection and/or thermal Marangoni convection.

The temperature dependence of surface tension was described by Straub[2] and Larkin.[3] At a liquid–vapor interface, attractive forces among liquid molecules cause surface tension effects. These interfacial tension forces increase or decrease with temperature, depending on the working fluids. In most cases, higher temperatures cause a reduction in strength of the intermolecular forces that bind the liquid together at the surface. The surface tension consequently decreases and becomes equal to zero at a critical temperature T_{crit}. If a temperature gradient is present at the surface, local stresses diminish toward the hot side and intensify toward the cold side. The surface tension variation induces a "tank-treadlike" motion of the vapor–liquid interface that, owing to the no-slip condition, causes a convective flow tangential to the interface. For the case of a bubble affixed to a heated surface, the thermocapillary or Marangoni convection can influence the wall heat transfer by acting as a pump that transports hot fluid near the wall into the cool bulk liquid, as depicted in Figure 1.

For Marangoni convection around a bubble of radius R_b within a channel of height H, the mass and heat transport mechanisms are characterized by the Prandtl and Marangoni numbers, defined, respectively, as[4–6]:

$$\mathrm{Pr} = \frac{\upsilon}{\alpha} \tag{1}$$

$$Ma = -\left(\frac{\partial \sigma}{\partial T}\right) \times \frac{T_h - T_c}{\mu \alpha} \times \frac{R_b^2}{H} \tag{2}$$

The Prandtl number represents the ratio of viscous to thermal diffusivity in the fluid, and may be assumed constant for a particular liquid if variations in viscosity and thermal diffusivity with temperature can be neglected, as is the case in this study. The Marangoni number represents the ratio of heat transfer by convection to that by conduction and is synonymous with the Peclet number. In experimental investigations, *Ma* is typically varied by changing the temperature difference within the system or by varying the height of the test domain channel. The latter method is sometimes the preferred approach as it prohibits any change in thermophysical conditions due to changing temperatures.

Many practical applications require that large amounts of heat be transferred quickly, efficiently, and with small temperature differences. Evaporation and condensation offer these desirable qualities and have thus been investigated to such an extent that they are used widely in countless technologies. However, owing to the complexity of the boiling and

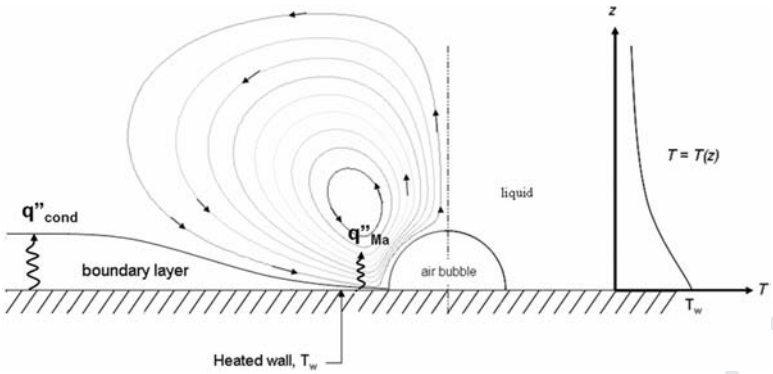

Figure 1. Surface-tension-induced flow around an air bubble at a heated wall.

condensation phenomena, the mechanisms of heat transfer are still poorly understood in the sense that predictive capabilities of theories and empirical correlations break down quickly once outside the parameter range in which they were developed.[7,8] For both terrestrial and space applications, research has indicated that the often neglected Marangoni convection may play an important role in the heat transfer during phase change processes.[2,9,10]

Thermocapillary convection has been the subject of some experimental work. Much of the recent literature focuses on flow analysis techniques and flow imaging of thermocapillary convection. Wozniak and colleagues[11–13] utilized particle-image-velocimetry and liquid-tracer techniques as well as interferometry to investigate the flow field resulting from the presence of a bubble in a fluid test cell with an applied temperature gradient under both terrestrial and microgravity conditions. Priede *et al.*[14] studied the effect of a free-surface contaminant in liquid semiconductors, highlighting an increase in surface tension with temperature, which resulted in an anomalous flow direction. There have also been analytical studies of thermocapillary convection concerned specifically with the temperature–velocity coupling at low Marangoni numbers.[15,16]

Young *et al.*[17] were the first to examine the effect of spherical free surfaces in the presence of a temperature gradient. They discovered that small air bubbles in a liquid sample could be held stationary or even driven against gravity with a sufficiently strong temperature gradient in the direction adverse to gravity. This was attributed to the variation in surface tension along the bubble surface, a condition caused by variations in the temperature field of the fluid. Some years later, McGrew *et al.*[18] argued that high boiling heat transfer rates are due to intense vapor bubble agitation of the liquid boundary layer close to the heating surface and bulk liquid disturbance due to bubble detachment from the surface. Utilizing tracer particles to observe the flow pattern around air bubbles placed on the heating surface and vapor bubbles produced during boiling, they conducted experiments in which the liquid was heated from above and cooled from the bottom, with slowly increasing heat flux levels. The flow profiles were identical for both air and vapor bubbles. They concluded that Marangoni convection would occur around any bubble present in a region subjected to a temperature gradient. They also suggested that this served as a primary factor in the heat transfer mechanism in those situations in which bubbles remained attached to the surface for relatively long periods of time.

For the case of a bubble affixed to a heated surface, Larkin[3] was likely the first to investigate the contribution of Marangoni convection to local heat transfer, obtaining time-dependent numerical solutions of flow and temperature fields for varying Prandtl and Marangoni numbers. The liquid was seen to move toward the

wall before being dragged along the bubble, finally leaving the bubble as a jet, the strength of which increased with increasing Marangoni number. Larkin investigated the influence of the surface-tension-driven flow on the Nusselt number, concluding that above a Marangoni number of 10^5, an increase in the rate of heat transfer of 30% was achievable. It was assumed that until this critical Marangoni number was reached, thermocapillary convection was not an important heat transfer mechanism. Unfortunately, owing to computational limitations of the time, Larkin was unable to continue the solution to steady state.

Later, Straub *et al.*[9] produced surprising results that indicated that the heat transfer coefficients measured for nucleate boiling in microgravity were similar in magnitude to those measured for terrestrial gravity. Since the microgravity experiments rule out buoyant natural convection as a heat transfer mechanism in the regions on the heated surface where bubble activity is not influential, Straub *et al.* proposed that the results could be attributed to the presence of thermocapillary convection.

Arlabosse *et al.*[5] investigated experimentally the contribution of Marangoni convection to heat transfer around bubbles attached to a heated surface within a channel. A test cell consisting of an upper heated flat plate, a lower cooled plate and plexiglass walls enclosed a silicone oil layer, into which an air bubble was injected and maintained on the upper heated surface. Tests were carried out for Prandtl numbers of 220, 440, and 880, and for a range of Marangoni numbers from 0 to 600. From the results obtained, it was determined that the ratio of heat transfer by Marangoni convection to that solely by conduction was well correlated by the relation

$$\frac{q''_{Ma}}{q''_{cond}} = 1 + 0.00841Ma^{0.5} \qquad (3)$$

In a similar study, Reynard *et al.*[8,19] performed experiments on test fluids of silicone oil with Prandtl numbers of 16.3 and 228 and FC-72 of Prandtl number 12.3, investigating the onset of the 3D oscillatory thermocapillary convection and the effect of test cell height.

Petrovic *et al.*[10] carried out experiments in order to examine the contribution of Marangoni convection to the rate of heat transfer in subcooled nucleate pool boiling using distilled water heated on a copper heater surface at atmospheric pressure and subcooling levels of 40°, 50°, 60°, and 70°C. The surface heat flux was incrementally increased from zero to a value sufficiently high to induce nucleate boiling. As the surface heat flux was increased for fixed liquid subcooling, the surface temperature continually increased and buoyant natural convection was the sole mechanism of heat transfer. However, at a critical surface heat flux, large and stationary air bubbles formed spontaneously Q1 on the surface with a significant increase in the heat transfer coefficient. The heat transfer mechanism was determined to be Marangoni convection and the heat transfer measurements were in agreement with the relationship proposed by Arlabosse *et al.*[5] for air bubbles of similar size, albeit in silicone oils.

Currently there is still very little quantitative information regarding the influence of Marangoni convection on the heat transfer that is due to bubbles fixed to heated surfaces. The objective of this paper is to provide preliminary numerical results that quantify the influence of Marangoni convection on the local and surface average wall heat transfer. With the view of developing the model for more complex situations such as nucleate pool boiling, this study considers the simplified case of a 2.0-mm-diameter stationary and hemispherical air bubble immersed in silicone oil. The simulated test vessel consists of two isothermal surfaces spaced 5 mm apart and the simulations are carried out in microgravity.

Mathematical Formulation

Since it is not driven by a gravitational field, much of the work done on Marangoni

convection is concerned with its possible application to thermal management in space applications. According to Bhunia and Kamotani,[20] two-phase liquid control systems have been identified as a superior alternative to single-phase pumped liquid loops to meet the rising power demand for spacecraft thermal management. It is, however, impossible to separate the effects caused simultaneously by buoyancy and surface tension convection in experiments on earth. Owing to the high cost and limited availability of microgravity experimentation, much of the work concerning thermocapillary convection has been implemented by numerical methods.[1–3,21,22] The accurate description of flows driven by surface tension gradients along an interface generally requires the solution of the full three-dimensional nonlinear equations of free-surface hydrodynamics.[22]

For the problem considered here, the procedure involves solving simultaneously the coupled equations of fluid mechanics and heat transfer. For low enough Marangoni numbers it is known that the resulting flow field is symmetric about the vertical bubble axis above the bubble centerline. Thus, a complicated and computationally expensive full 3D model is not utilized in favor of 2D axisymmetric formulations. From experimental observations,[5,6,19] it is known that a strong jet-type flow is produced immediately after the appearance of a bubble on the surface. The liquid is projected vertically away from the center of the bubble with the colder liquid being drawn inward toward the heated surface and the regions of the bubble close to the heated surface.

The following work involves the numerical simulation of Marangoni convection and focuses on the problem of thermocapillary flow induced by the presence of a hemispherical bubble attached to a heated planar surface. A two-dimensional axisymmetric model of the problem was formulated using the commercial software package FLUENT. The governing equations that were solved were the steady-state continuity, momentum, and energy equations:

Continuity:

$$\frac{\partial}{\partial x}(\rho v_x) + \frac{\partial}{\partial r}(\rho v_r) + \frac{\rho v_r}{r} = 0. \tag{4}$$

Energy:

$$v_x \frac{\partial T}{\partial x} + v_r \frac{\partial T}{\partial r} = \alpha \left(\frac{\partial^2 T}{\partial x^2} + \frac{1}{r}\frac{\partial T}{\partial r} + \frac{\partial^2 T}{\partial r^2} \right). \tag{5}$$

Axial momentum:

$$\frac{1}{r}\frac{\partial}{\partial x}\left(r\rho v_x^2\right) + \frac{1}{r}\frac{\partial}{\partial r}\left(r\rho v_x v_r\right) = -\frac{\partial p}{\partial x} + \frac{1}{r}\frac{\partial}{\partial x} \times \left[r\mu \left(2\frac{\partial v_x}{\partial x} - \frac{2}{3}(\nabla \cdot \vec{v}) \right) \right] + \frac{1}{r}\frac{\partial}{\partial r} \times \left[r\mu \left(\frac{\partial v_x}{\partial r} + \frac{\partial v_r}{\partial x} \right) \right]. \tag{6}$$

Radial momentum:

$$\frac{1}{r}\frac{\partial}{\partial x}\left(r\rho v_x v_r\right) + \frac{1}{r}\frac{\partial}{\partial r}\left(r\rho v_r^2\right) = -\frac{\partial p}{\partial r} + \frac{1}{r}\frac{\partial}{\partial x} \times \left[r\mu \left(\frac{\partial v_r}{\partial x} + \frac{\partial v_x}{\partial r} \right) \right] + \frac{1}{r}\frac{\partial}{\partial r} \times \left[r\mu \left(2\frac{\partial v_r}{\partial r} - \frac{2}{3}(\nabla \cdot \vec{v}) \right) \right] - 2\mu\frac{v_r}{r^2} + \frac{2}{3}\frac{\mu}{r}(\nabla \cdot \vec{v}). \tag{7}$$

Here

$$\nabla \cdot \vec{v} = \frac{\partial v_x}{\partial x} + \frac{\partial v_r}{\partial r} + \frac{v_r}{r}. \tag{8}$$

In accordance with previous numerical investigations on Marangoni convection, the following assumptions are made in the analysis:

1. Motion is 2D axisymmetric in cylindrical coordinates.
2. A bubble can be represented by a hemispherical interface.
3. Heat flux is zero at the bubble interface.
4. Incompressibility of the liquid (ρ = constant).
5. Constant physical properties [μ, $k \neq f(T, t \ldots)$ etc.].
6. Gravitational acceleration is zero.

Since this work is approximate and not an exact numerical simulation, it is important to briefly discuss the major assumptions that were made during the physical modeling of the problem, since they ultimately determine the usefulness of any conclusions that are drawn from the results. The assumption that the flow is 2D is valid since it has been established that unsteady oscillatory and 3D flow occurs at a critical Marangoni number, $Ma \sim 12{,}000$,[23] which is considerably higher than the maximum Marangoni number tested in this study.

Another major assumption is that the bubble interface maintained a spherical shape and did not deform from the presence of a pressure field. In order to determine the shape of the gas–liquid interface, two parameters are generally required[24]; the size of the bubble or drop and the contact angle. Experimental data concerning the material-dependent static contact angle for a 1.0-mm-radius air bubble immersed in silicone oil ($Pr = 82.5$) are not available. Thus, the concept of a macroscopic contact angle as discussed by Vafaei and Podowski[24] is used. In that study, the gas–liquid contact angles were influenced by size and external conditions.

An example of this type of analysis can been seen in the work of Arlabosse *et al.*,[5] who noted that for their experiments, up to a radius of 1.3 mm, the bubble maintained a spherical shape. Under similar conditions, albeit at a lower Prandtl number, the bubble radius for this numerical study is 1.0 mm. Furthermore, in the work of Arlabosse *et al.* the macroscopic contact angle increased from 52° to 71.5° for bubbles of equivalent radius 2.0 mm and 1.5 mm, respectively. This resulted in Bond numbers of approximately $Bo = 0.64$ and $Bo = 0.36$ for the 2.0 mm and 1.5 mm bubbles, respectively, which suggests that bubble size influences the contact angle and at lower values of the Bond number, bubbles tend toward a hemispherical shape. The Bond number for this study under conditions similar to those in Arlabosse *et al.*[5] is approximately $Bo = 0.2$, which suggests that a macroscopic contact angle of 90° is reasonable. As a means of provisionally investigating the influence of the contact angle, some simulations were conducted for a 1.0-mm bubble with a contact angle of approximately 80°. The difference in the resulting heat transfer enhancement was found to be insignificant compared with the hemispherical bubble. Moreover, the present simulations are also performed under microgravity conditions, so there is no deformation of the interface from gravitational effects. Consistent with simulations performed by Straub[2] and Larkin,[3] a hemispherical bubble shape is employed.

Another key assumption that was made in developing the model was that no heat transfer occurred across the bubble interface. Thus the results presented herein are not immediately applicable to nucleate pool boiling circumstances, where evaporation at the interface creates a much more uniform temperature at the surface and thus acts to suppress the thermocapillary flow. The actual mechanism for the onset of thermocapillary flow during boiling is uncertain, although evidence seems to indicate that it is caused by variation in the evaporation and condensation heat transfer coefficient at the vapor–liquid interface,[25–27] which can possibly arise from the presence of noncondensable gas.[25,28,29] Thus the assumption is consistent with the Marangoni heat transfer regime discovered by Petrovic *et al.*,[10] where air bubbles caused a significant enhancement in the heat transfer even when the heated wall temperature was below the saturation temperature. The work is also qualitatively comparable to the situation of gas-saturated liquids, for example, the experimental results of Henry.[29]

Following these assumptions, it is possible to model thermocapillary convection caused by the bubble without modeling motion within the bubble itself. The bubble is represented by a boundary upon which a Marangoni stress is applied.

The model domain is shown in Figure 2. A bubble of radius 1.0 mm is placed at the center of the coordinate plane. The vertical wall denoted "*sym*" signifies the axis of symmetry.

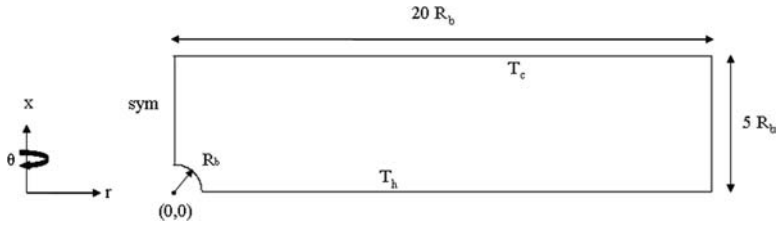

Figure 2. Model domain schematic.

TABLE 1. Properties of Silicone Oil 7.5cSt

ρ (k·gm^{-3})	υ (m^2·s^{-1})	k (W·m^{-1}K^{-1})	C_p (J·kg^{-1}K^{-1})	$d\sigma/dT$ (N·m^{-1}K^{-1})
930	7.5e−6	0.125	1480	−5.8e−5

The two horizontal walls are separated by a distance H, which is equivalent to five times the bubble radius. The upper wall is no-slip, constant temperature:

$$\vec{v} = 0, \quad T = T_0 \tag{9}$$

and is maintained at 300 K for all simulations. The lower horizontal wall is also no-slip, constant temperature:

$$\vec{v} = 0, \quad T = T_0 \tag{10}$$

and the temperature of this wall is changed from one simulation to the next. The vertical wall placed 20 bubble radii from the center of the bubble has a no-slip, adiabatic condition:

$$\vec{v} = 0, \quad \vec{n} \cdot (k \nabla T) = 0 \tag{11}$$

The bubble surface is comprised of a slip condition, an adiabatic condition, and a directly applied Marangoni stress:

$$\vec{n} \cdot \vec{v} = 0, \quad \vec{n} \cdot (k \nabla T) = 0 \tag{12}$$

$$\vec{\tau} = \frac{d\sigma}{dT} \nabla T, \tag{13}$$

which relates the shear stress on the surface to the temperature derivative of surface tension. The test fluid was selected to have the same properties as silicone oil of kinematic viscosity 7.5cSt. The relevant physical properties are given in Table 1.

The commercial code FLUENT release 6.2.16 was utilized to solve the problem. From calculations of the Reynolds number, it was known that the resulting flow would be laminar. The segregated solver was selected on the basis of computing power. The numerical scheme adopted was second order upwind. Solutions were carried out for temperature differences of 50, 40, 30, 20, 10, and 1 Kelvin, corresponding to Marangoni numbers of 915, 732, 550, 366, 183, and 18.3, respectively. Grid independence was achieved by increasing the number of quadrilateral cells from 1260 to 81,000, plotting the convergence of certain parameters of interest such as free surface velocity, and tracking global parameters such as total rate of heat transfer through the system.

Numerical Validation

The correctness of the physical modeling and numerical solution technique has been confirmed by comparing the simulations against existing numerical work as well as some experimental data. In order to establish confidence in the accuracy of the CFD software used in this investigation, the benchmark numerical data for thermocapillary flow in a rectangular enclosure provided by Zebib *et al.*[30] were reproduced and excellent agreement is shown in Figure 3 for a sufficient range of Reynolds numbers.

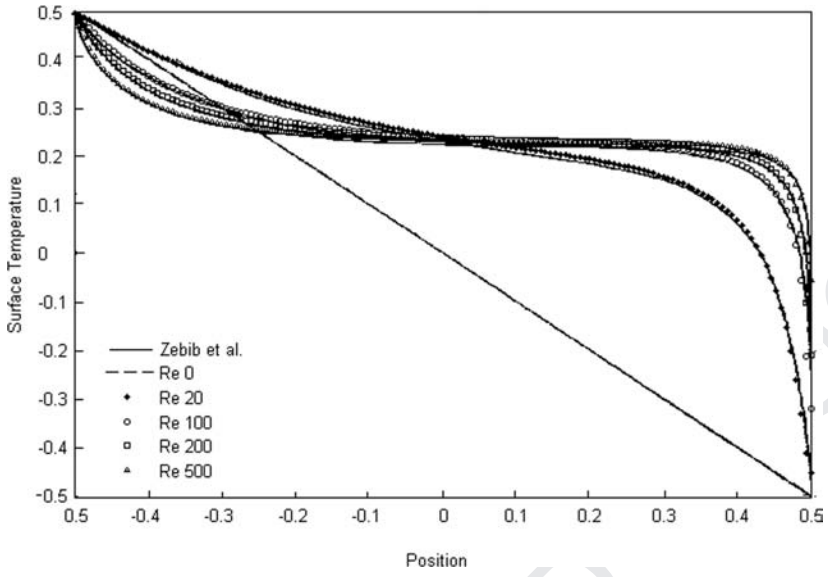

Figure 3. Free surface temperature at $Pr = 50$ and $Re = 0$, 20, 100, 200, and 500.

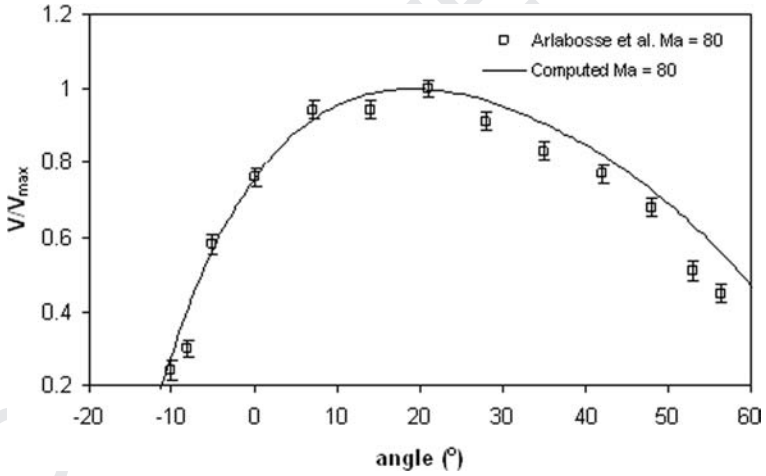

Figure 4. Nondimensional velocity profile along the bubble interface for $Pr = 220$, $Bo = 0.35$, and $Ma = 80$.

Figures 4 and 5 show the comparison of the numerical simulations with the experimental data provided by Arlabosse *et al.*[5] Their experimental data were obtained at terrestrial gravity for air bubbles affixed on the underside of a heated wall with the cooled wall below, such that buoyancy acted in opposition to the thermocapillary convection. In order to simulate this condition, the Boussinesq approximation was applied within FLUENT as a body force F_B on the right-hand side of the axial momentum equation [Eq. (6)] and simulations for $Bo = 0.35$, $Pr = 220$, and $Ma = 80$ were carried out, where the Bond number is calculated from the expression

$$Bo = \frac{\rho_{oil}\beta_{oil} g R_b^2}{\dfrac{\partial \sigma}{\partial T}} \tag{14}$$

As shown in Figure 4 the agreement between the measured nondimensional interface

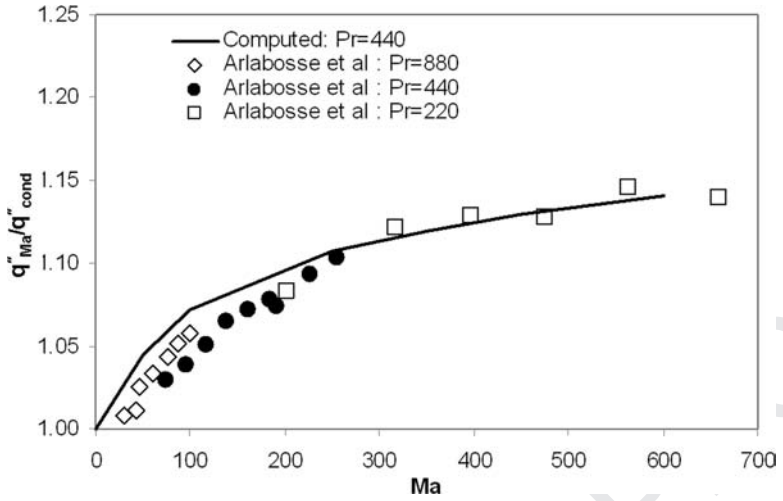

Figure 5. Change in the ratio of heat transferred with and without the bubble for $Bo \approx 0.25$.

velocity and the simulation is quite good. Any deviations are possibly due to small variations in the thermophysical properties with temperature or the small difference in shape of the bubble in Arlabosse *et al.*,[5] which, although very nearly hemispherical with a contact angle of 71.5°, is slightly ellipsoidal.

Since the primary objective of this investigation is to quantify the local heat transfer behavior in the vicinity of bubbles affixed to a heated surface, it is imperative that the numerical simulations be validated against available empirical heat transfer data. Utilizing a heat flux sensor glued to the cold wall below the bubble, Arlabosse *et al.*[5] quantified the increase in the average heat flux across the sensor situated on the wall opposite to that of the bubble. Comparison between the experimental and numerically simulated heat flux enhancement ratio shown in Figure 5 is acceptable. For this comparison, the net power across a fixed area of 57 mm^2 was chosen to determine the heat flux for the simulations. This is the same, typical, active area of 10×10 mm^2 heat flux sensors as was used in that work. It should be noted that the Bond number for the experiments was $Bo = 0.25$, which corresponds to the small bubbles that retain their spherical shape,[5] which is consistent with the simulated geometry.

Results and Discussion

Marangoni Number = 915

Figure 6 shows the temperature and velocity profile for $Ma = 915$. For the fixed geometry, this was the largest Marangoni number simulated and corresponds to the largest temperature differential across the upper and lower plates. The vector plot details the motion of the fluid. The flow field consists of a major vortex that recirculates colder fluid from the upper region, pulling it toward the hot surface to the point where the bubble meets the heated wall. Interestingly, the fluid begins to accelerate before reaching the vapor–liquid interface. The fluid is then dragged along the bubble surface. In this region the highest velocities are found as the fluid is accelerated by surface tension effects. The fluid then leaves the bubble as a jet, which decelerates with increasing distance from the bubble. This type of flow pattern has been seen in various experiments.[5,6,19]

The focus of this paper is to quantify the contribution of Marangoni convection to local heat transfer from the heated surface in the vicinity of the bubble. Initially, simulations were carried out over a similar domain in the absence of the bubble to predict the heat transfer due to pure molecular diffusion and establish a "base-line"

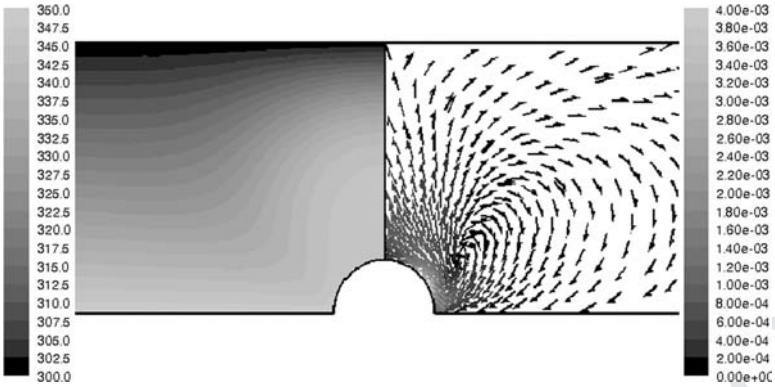

Figure 6. Temperature contours/velocity vectors for $Ma = 915$.

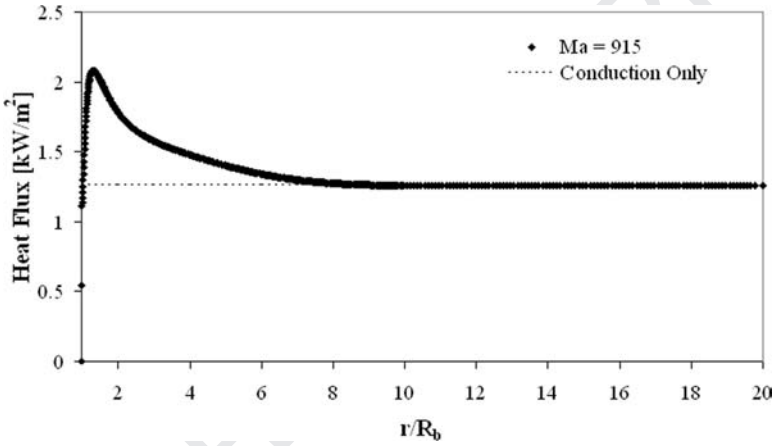

Figure 7. Surface heat flux along the heated wall.

to which subsequent conditions can be compared. Consistent with analytical predictions, the heat flux along the channel walls was constant in the absence of the bubble.

Figure 7 illustrates the heat flux profile along the heated wall caused by Marangoni convection for $Ma = 915$. The heat flux from pure conduction in the absence of the bubble is depicted by the horizontal dashed line. It is evident that the presence of the bubble causes a sharp increase in surface heat transfer in the immediate vicinity of the bubble. The peak heat flux occurs at a distance of just over two radii from the bubble. Moving further away from the bubble in the radial direction, the surface heat transfer decreases and eventually approaches the pure conduction heat flux as expected. Most importantly, it is noted that significant heat transfer enhancement is observed over a considerable distance from the contact line, in this case nearly $r \sim 8R_b$, which is significant.

By magnifying the region immediately adjacent to the triple interface, a sharp rise in heat flux is predicted. This trend is detailed in Figure 8. In an effort to understand the phenomenon the triple contact point was scrutinized more closely with regard to the flow regime in the area. In particular, the vorticity, which is extreme in this region since the fluid rapidly changes from a nearly horizontal to a nearly vertical flow direction, is considered. Figure 9 shows a magnified view of the vorticity contours in a region near the triple contact line. Evidently, in the region where the bubble meets the wall there is a relatively small zone of high vorticity. Although the flow velocity is

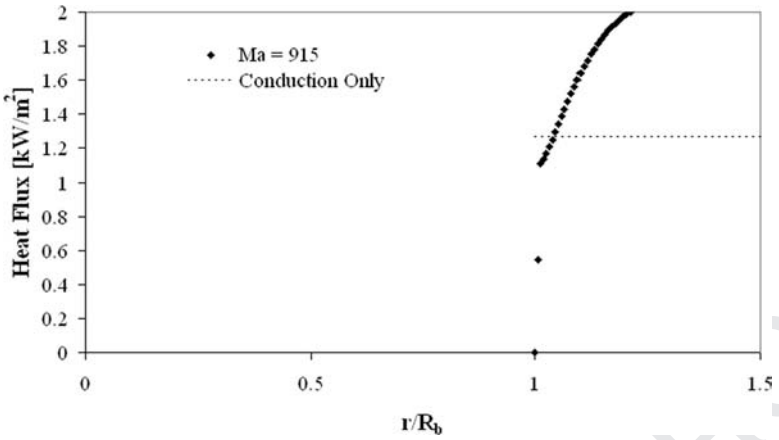

Figure 8. Surface heat flux near the triple interface.

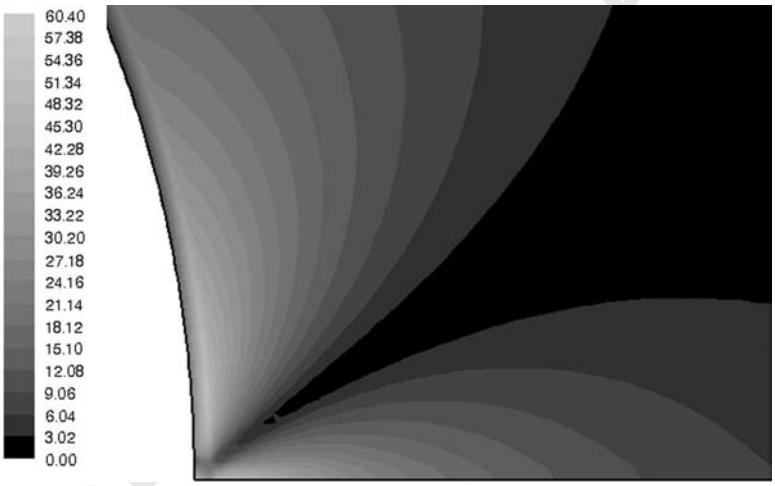

Figure 9. Vorticity near the triple interface.

quite low in this region, the increased mixing associated with the high vorticity has the effect of increasing the rate of heat transfer. In the near region, the vorticity drops disproportionately to the increase in bulk convection. After this point the heat transfer begins to rise considerably as the primary and largely irrotational vortex becomes the primary mechanism for heat transport. This is highlighted by the velocity vector plot shown in Figure 10. The no-slip wall boundary condition ensures that minimal fluid velocities are found near the triple interface. The geometry of the bubble causes a rotation in the fluid as it approaches the bubble. The no-slip point between the bubble and the wall results in a sudden and sharp rotation of the fluid, resulting in high vorticity in this region. By comparing the vorticity and velocity plots it is evident that the region of low vorticity corresponds to the region where the velocity vectors travel mostly in the same direction. This region represents the bulk cooler fluid being recirculated from above by thermocapillary convection.

Effect of Marangoni Number on Flow and Heat Transfer

Velocity and temperature data have been obtained for each of the six test cases.

Figure 11A–E show the temperature contours and velocity streamlines for different

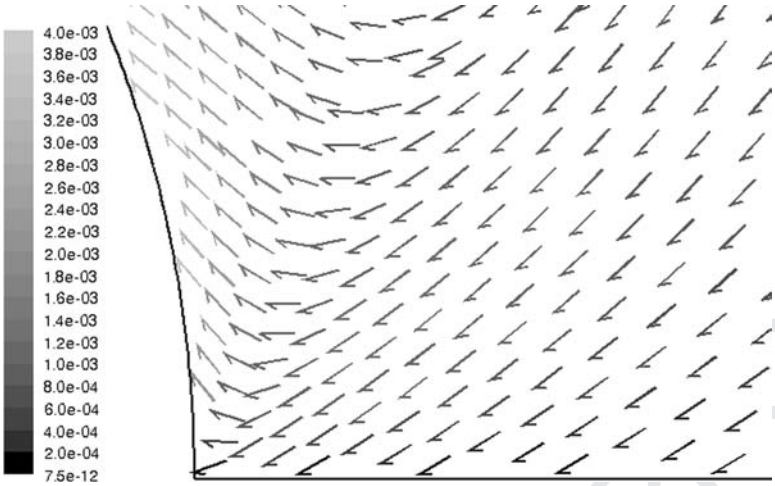

Figure 10. Velocity near the triple interface: (**A**) $\Delta T = 50$ K, $Ma = 915$; (**B**) $\Delta T = 40$ K, $Ma = 732$; (**C**) $\Delta T = 30$ K, $Ma = 550$; (**D**) $\Delta T = 20$ K, $Ma = 366$; (**E**) $\Delta T = 10$ K, $Ma = 183$.

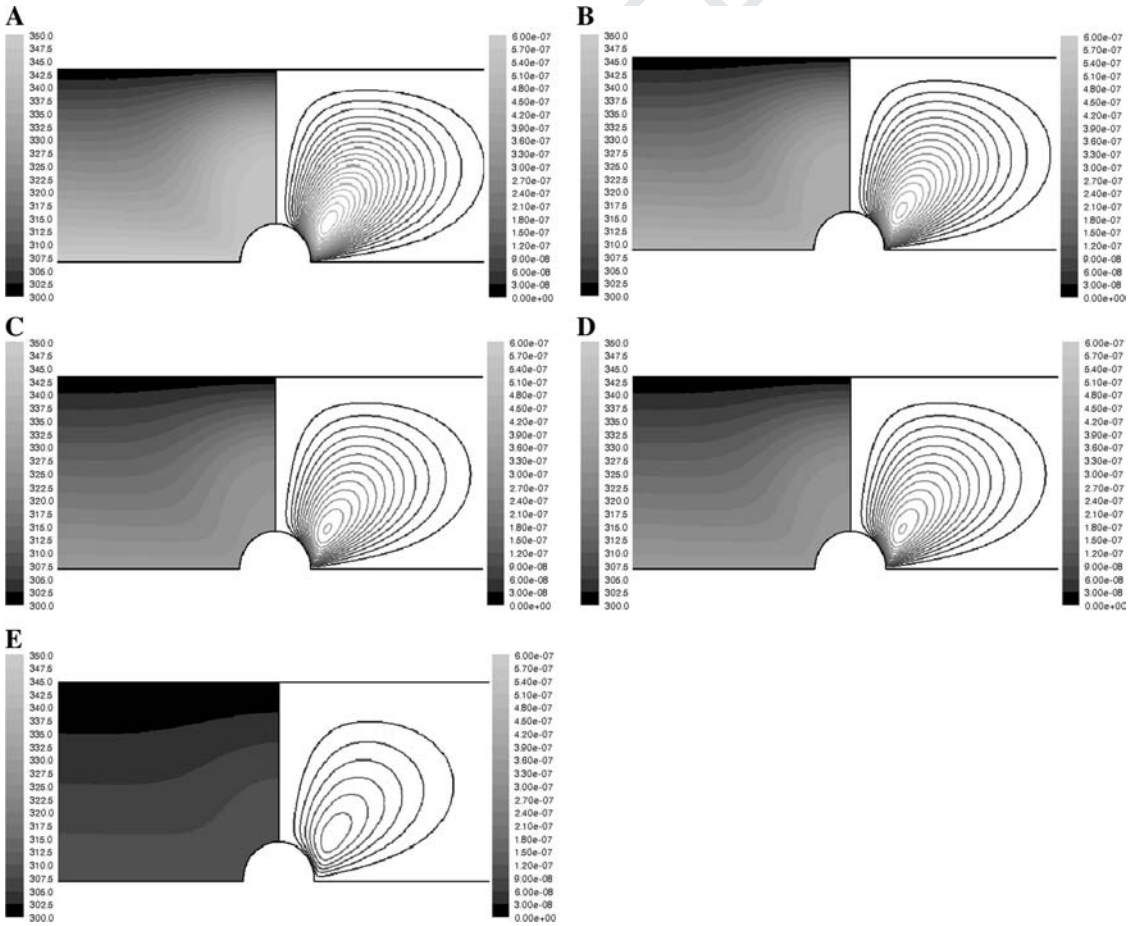

Figure 11. (**A–E**) Temperature contours/velocity streamlines for varying Marangoni number.

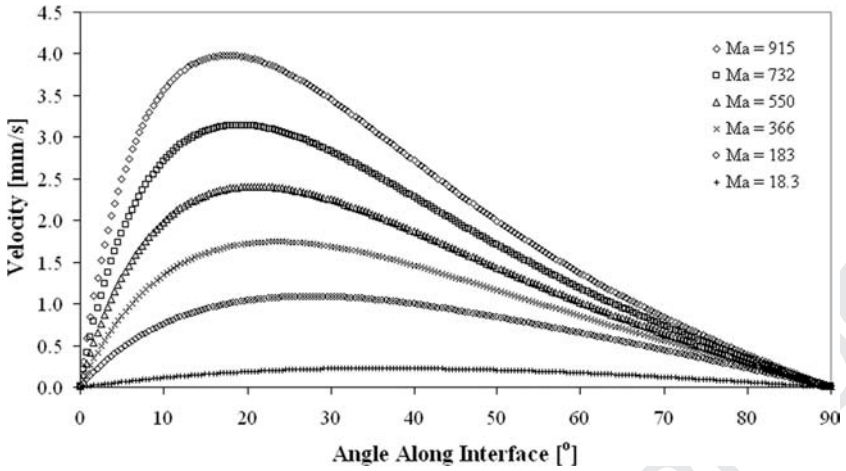

Figure 12. Velocity along bubble for varying Marangoni number.

Marangoni numbers. By applying the same temperature and stream function scales to each plot, it is evident that with decreasing temperature the thermocapillary effect decreases in strength. The plot for $Ma = 18.3$ is not presented as there is little distinguishable difference for the selected grayscale. In particular, the intensity of the jetlike flow diminishes with decreasing Marangoni number. The figure also shows the temperature contours, which are characteristic of this phenomenon. In the absence of the bubble, the contours would form parallel vertical lines. This scenario is characteristic of conduction only flows and would also be seen far from the bubble. In the vicinity of the bubble, the temperature contours bend toward the heated wall. This is caused by the flow of cooler liquid toward the hot wall. The liquid jet, in flowing outward from the apex of the bubble, causes the temperature contours to project outward. The proximity of the upper wall, which has a no-slip condition, limits the extent the jet can travel in this scenario. From these images, it is evident that the thermocapillary flow field is increasing heat transfer by stripping it from the wall in the vicinity of the bubble and convecting it into the bulk region above the bubble.

Figure 12 shows the velocity profile around the bubble for different Marangoni numbers. Angles are computed from the heated wall to the center point of the bubble. The angle corresponding to maximum velocity decreases slightly with increasing Marangoni number. A possible explanation for this may be that with greater Marangoni number the surface tension gradients along the surface of the bubble are steeper, which accelerates the fluid moving toward the triple interface. The cooler fluid then encounters a region of high vorticity at the triple interface, which could cause the local fluid velocity to increase.

Enhancement of Heat Transfer

The enhancement of local heat transfer is best expressed as the ratio of heat transfer in the presence of Marangoni convection to that by pure molecular diffusion. Figure 13 shows this enhancement ratio for increasing Marangoni number. For a $Ma = 18.3$, there is a large peak immediately at the triple interface. This behavior is in agreement with that seen previously in Figure 7 for $Ma = 915$. In this case, however, the high vorticity causes a large increase in the relative heat transfer near the triple interface, but the interface fluid motion is not strong enough to cause significant bulk motion of the fluid. As expected, the maximum enhancement factor increases with increasing Marangoni number, reaching over 65% for $Ma = 915$. Interestingly, all curves between $Ma = 18.3$ and

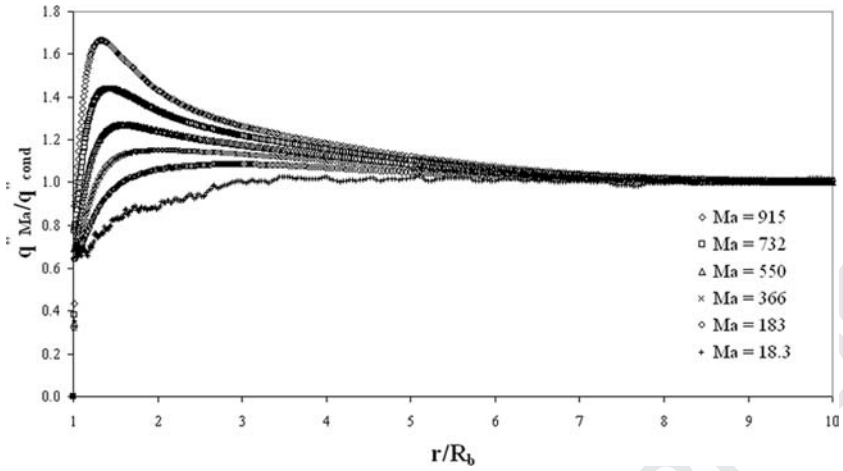

Figure 13. Hot wall heat flux enhancement.

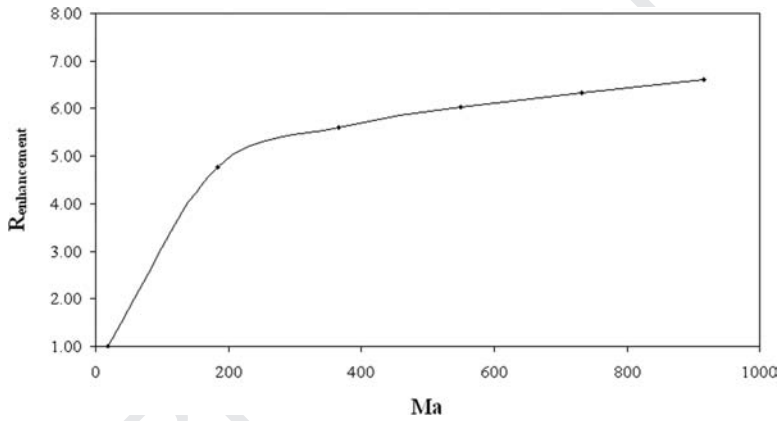

Figure 14. Enhancement radius vs. Marangoni number.

$Ma = 915$ seem to converge to their q_{cond} value at almost the same radial location of approximately $r = 7R_b$. Consequently, an enhancement range may be roughly defined. The enhancement region appears to be nearly constant for a particular range of Marangoni numbers tested, but may depend on the definition of the Marangoni number itself, in particular in the choice of length scale. Furthermore, in this study, the Marangoni number was chosen to include the height of the domain, H, as has been used in experimental practices.[5,8,19] The enhancement region may be defined in terms of a radius measured outward from the center point of the bubble. The enhancement criterion for this investigation is defined as the location at which the heat transfer due to Marangoni convection falls to within 5% of the value due to pure conduction, or equivalently

$$R_{enhancement} = \left.\frac{r}{R_b}\right|_{1.05\times q''_{cond}} \tag{15}$$

Figure 14 shows the enhancement radius against Marangoni number. At the low values of Ma there is a steep increase in the effective radius of enhancement, until the curve begins to level off at $Ma \sim 200$. This suggests that large Marangoni numbers are not required for the influence of the bubble to be felt almost three diameters away. Although the enhancement radius continues to increase with increasing Marangoni number, the increase is not profound. Indeed the trend suggests that the

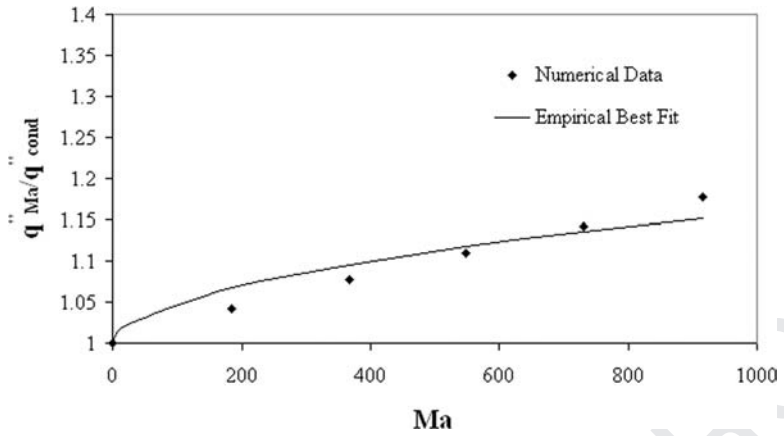

Figure 15. Heat transfer enhancement vs. Marangoni number.

effective radius of enhancement approaches an asymptotic value of approximately $r \sim 7R_b$. Furthermore, the enhancement radius also implies that with increasing Marangoni number, the size of the main vortex does not increase greatly, but perhaps its intensity does, thus increasing local heat transfer. By defining an effective radius and corresponding area of heat transfer such that

$$R_{eff} = 7R_b, \quad A_{eff} = \pi\left(R_{eff}^2 - R_b^2\right), \quad (16)$$

the increase in total heat transfer relative to conduction can be expressed in terms of this value.

Figure 15 charts this increase versus Marangoni number. Following experimental investigations by Arlabosse *et al.*[5] and Petrovic *et al.*,[10] a similar heat exchange correlation was derived:

$$\frac{q''_{Ma}}{q''_{cond}} = 1 + 0.005Ma^{0.5} \quad (17)$$

When $Ma = 0$ (without any temperature gradient or without a bubble) $q''_{Ma}/q''_{cond} = 1$, which corresponds to conductive heat transfer. It must be noted that the authors referenced in Arlabosse *et al.*[5] studied the effective heat transfer on the cooler wall away from the bubble. The coefficient also depends on the choice of affected area.

Conclusions and Outlook

The influence of the Marangoni number on the local heat transfer in the vicinity of an air bubble with radius of 1 mm was investigated numerically for a liquid silicone oil layer ($Pr = 82.5$) of a constant depth of 5 mm, for Marangoni numbers in the range $0 \leq Ma \leq 915$ under microgravity conditions. The increase in the local and surface average heat flux on the wall to which the bubble is attached was computed and it was determined that, compared to pure conduction, thermocapillary convection enhanced the local heat flux more than 65%. Q4 Furthermore, the enhanced heat transfer penetrated a distance of approximately seven bubble radii. The numerical results indicate that the ratio of Marangoni heat transfer to conduction over the area of enhancement changes approximately with the square root of the Marangoni number. For the range of Marangoni numbers tested, an 18% improvement in the average heat transfer in the vicinity of the bubble was calculated.

In the near term simulations are planned to cover a greater range of Marangoni and Rayleigh numbers, including full 3D models, so that unsteady and oscillatory thermocapillary flow can be investigated. Since understanding of the heat transfer mechanisms during nucleate pool boiling is the ultimate goal of this research, the adiabatic boundary condition will

be lifted and replaced with appropriate evaporation and condensation boundary conditions, perhaps similar to those suggested by Raj and Kim.[25] In the longer term it is expected that the contribution of Marangoni convection to heat transfer during rapid bubble growth in boiling will be quantified.

Acknowledgments

This work was supported in part by the Irish Research Council for Science, Engineering and Technology (IRCSET) Embark Initiative.

Conflicts of Interest

The authors declare no conflicts of interest.

References

1. Betz, J. & J. Straub. 2001. Numerical and experimental study of the heat transfer and fluid flow by thermocapillary convection around gas bubbles. *Heat Mass Trans./Waerme- und Stoffuebertragung* **37:** 215–227.
2. Straub, J. 1994. Role of surface tension for two-phase heat and mass transfer in the absence of gravity. *Exp. Thermal Fluid Sci.* **9:** 253–273.
3. Larkin, B.K. 1970. Thermocapillary flow around hemispherical bubble. *AIChE J.* **16:** 101–107.
4. Arlabosse, P., N. Lock, M. Medale & M. Jaeger. 1999. Numerical investigation of thermocapillary flow around a bubble. *Phys. Fluids* **11:** 18–29.
5. Arlabosse, P., L. Tadrist, H. Tadrist & J. Pantaloni. 2000. Experimental analysis of the heat transfer induced by thermocapillary convection around a bubble. *J. Heat Trans.* **122:** 66–73.
6. Reynard, C., R. Santini & L. Tadrist. 2001. Experimental study of the gravity influence on the periodic thermocapillary convection around a bubble. *Exp. Fluids* **31:** 440–446.
7. Marek, R. & J. Straub. 2001. The origin of thermocapillary convection in subcooled nucleate pool boiling. *Int. J. Heat Mass Trans.* **44:** 619–632.
8. Reynard, C., R. Santini & L. Tadrist. 2003. Experimental study of fluid-wall heat transfer induced by thermocapillary convection: Influence of the Prandtl number. *C. R. Acad. Sci., Ser. IIb: Mec.* **331:** 237–244.
9. Straub, J., M. Zell & B. Vogel. 1993. What we learn from boiling under microgravity. *Microgravity Sci. Tech.* **6:** 239–247.
10. Petrovic, S., T. Robinson & R.L. Judd. 2004. Marangoni heat transfer in subcooled nucleate pool boiling. *Int. J. Heat Mass Trans.* **47:** 5115–5128.
11. Wozniak, G. 1999. Optical whole-field methods for thermo-convective flow analysis in microgravity. *Meas. Sci. Technol.* **10:** 878–885.
12. Wozniak, K., G. Wozniak & T. Roesgen. 1990. Particle-image-velocimetry applied to thermocapillary convection. *Exp. Fluids* **10:** 12–16.
13. Wozniak, G. & K. Wozniak. 1994. Buoyancy and thermocapillary flow analysis by the combined use of liquid crystals and PIV. *Exp. Fluids* **17:** 141–146.
14. Priede, J., A. Cramer, A. Bojarevics, *et al*. 1999. Experimental and numerical study of anomalous thermocapillary convection in liquid gallium. *Phys. Fluids* **11:** 3331–3339.
15. Balasubramaniam, R. & R.S. Subramanian. 2004. Thermocapillary convection due to a stationary bubble. *Phys. Fluids* **16:** 3131–3137.
16. Balasubramaniam, R. & R.S. Subramanian. 2003. Thermocapillary convection in a spherical container due to a stationary bubble. *Adv. Space Res.* **32:** 137–142.
17. Young N.O., J.S. Goldstein & M.J. Block. 1959. The motion of bubbles in a vertical temperature gradient. *J. Fluid Mech.* **6:** 350–356.
18. McGrew J.L., F.L. Bamford & T.R. Rehm. 1966. Marangoni flow: An additional mechanism in boiling heat transfer. *Science* **153:** 1106–1107.
19. Reynard, C., M. Barthes, R. Santini & L. Tadrist. 2005. Experimental study of the onset of the 3D oscillatory thermocapillary convection around a single air or vapor bubble: Influence on heat transfer. *Exp. Thermal Fluid Sci.* **29:** 783–793.
20. Bhunia, A. & Y. Kamotani. 2001. Flow around a bubble on a heated wall in a cross-flowing liquid under microgravity condition. *Int. J. Heat Mass Trans.* **44:** 3895–9905.
21. Morris, C.J. & B.A. Parviz. 2006. Self-assembly and characterization of Marangoni microfluidic actuators. *J. Micromech. Microeng.* **16:** 972–980.
22. Thess, A., D. Spirn & B. Juettner. 1997. Two-dimensional model for slow convection at infinite Marangoni number. *J. Fluid Mech.* **331:** 283–312.
23. Kassemi, M. & N. Rashidnia. 1996. Bubble dynamics on a heated surface. Presented at the *Third Microgravity Fluid Physics Conference*, Cleveland, Ohio.
24. Vafaei, S. & M. Z. Podowski. 2005. Theoretical analysis on the effect of liquid droplet geometry on contact angle. *Nucl. Eng Des.* **235:** 1293–1301,
25. Raj, R. & J. Kim. 2007. Thermocapillary convection during subcooled boiling in reduced gravity environments. Presented at the *Fifth Interdisciplinary Transport Phenomena: Fluid, Thermal, Biological, Materials and Space Sciences*. Bansko, Bulgaria.

26. Lu, J.F. & X.F. Peng. 2007. Bubble jet flow formation during boiling of subcooled water on fine wires. *Int. J. Heat Mass Trans.* **50:** 3966–3976.
27. Wang, H., X.F. Peng, D.M. Christopher, *et al*. 2005. Investigation of bubble-top jet flow during subcooled boiling on wires. *Int. J. Heat Fluid Flow* **26:** 485–494.
28. Barthes, M., C. Reynard, R. Santini & L. Tadrist. 2007. Non-condensable gas influence on the Marangoni convection during a single vapour bubble growth in a subcooled liquid. *Europhys. Lett.* **77:** 1–5.
29. Henry, C.D., J. Kim & J. McQuillen. 2006. Dissolved gas effects on thermocapillary convection during boiling in reduced gravity environments. *Heat Mass Trans.* **42:** 919–923.
30. Zebib, A., G.M. Homsy & E. Meiburg. 1985. High Marangoni number convection in a square cavity. *Phys. Fluids* **28:** 3467–3476.

Queries

Q1 Author: OK or 'an air bubble'?

Q2 Author: OK this way?

Q3 Author: There are no letters on the figure to correspond to a-e. Please provide another figure with labels.

Q4 Author: OK?